

Journal of  
**Applied Remote Sensing**

RemoteSensing.SPIEDigitalLibrary.org

**Assessment of human health impact  
from PM<sub>10</sub> exposure in China based  
on satellite observations**

Wen Wang  
Tao Yu  
Pubu Ciren  
Peng Jiang

# Assessment of human health impact from PM<sub>10</sub> exposure in China based on satellite observations

Wen Wang,<sup>a</sup> Tao Yu,<sup>a</sup> Pubu Ciren,<sup>a,b,\*</sup> and Peng Jiang<sup>a</sup>

<sup>a</sup>Renmin University of China, School of Environment and Natural Resources, Center for Spatial Information, 59 Zhongguancun Street, Beijing 100872, China

<sup>b</sup>IMSG at NOAA/NESDIS/STAR, 5825 University Research Center, Suite 3250, M Square, College Park, Maryland 20740, United States

**Abstract.** Assessment of human health impact from the exposure to PM<sub>10</sub> air pollution is crucial for evaluating environmental damage. We established an empirical model to estimate ground PM<sub>10</sub> mass concentration from satellite-derived aerosol optical depth and adopted the dose-response model to evaluate the annual average human health risks and losses related to PM<sub>10</sub> exposure over China from 2010 to 2014. Unlike the traditional human health assessment methods, which relied on the *in situ* PM<sub>10</sub> concentration measurements and statistical population data issued by administrative district, the approach proposed in this study obtained the spatial distribution of human health risks in China by analyzing the distribution of PM<sub>10</sub> concentration estimated from satellite observations and population distribution based on the relationship to the spatial distribution of land-use type. It was found that the long-term satellite observations have advantages over the ground-based observations in estimating human health impact from PM<sub>10</sub> exposure. © The Authors. Published by SPIE under a Creative Commons Attribution 3.0 Unported License. Distribution or reproduction of this work in whole or in part requires full attribution of the original publication, including its DOI. [DOI: [10.1117/1.JRS.9.096027](https://doi.org/10.1117/1.JRS.9.096027)]

**Keywords:** moderate resolution imaging spectroradiometer; human health assessment; distribution; PM<sub>10</sub>; aerosol optical depth.

Paper 15100 received Feb. 5, 2015; accepted for publication Jun. 18, 2015; published online Jul. 20, 2015.

## 1 Introduction

The impact on human health from exposure to particulate matter (PM) pollution is staggering. Studies from the World Health Organization (WHO) have shown that PM pollution contributed to ~3.2 million premature deaths and 7.4 million disability-adjusted life years in each year.<sup>1</sup> ~50% of them are from East and Southeast Asian countries, where PM pollution is at a more serious level.<sup>2</sup> It is worth noting that in China, among the largest 500 cities, only 1% of them are able to reach the air quality standards recommended by WHO, and seven of the world's ten most polluted cities are in China.<sup>3</sup> With the process of industrialization, high concentrations of PMs have gradually developed into a serious regional environmental problem.

Assessment of the human health impact caused by PM<sub>10</sub> exposure is important for evaluating environmental damage related to air pollution. PM<sub>10</sub> may make their way into human beings through respiration. Toxic substances attached to PM<sub>10</sub> particles could lead to a series of respiratory disease, cardiovascular disease, and increase the risks of cancer. However, even with the great potentials for affecting human health, risks assessment of PM<sub>10</sub> exposure in a large area over China is very scarce. Quantitative analysis of the human health risks and losses by PM<sub>10</sub> pollution in China can efficiently reflect the spatial distribution and variability of PM<sub>10</sub> concentration and exposure levels to the residents, as well as the risks of diseases. In addition, such studies would provide a scientific basis for estimating economic losses as a result of

---

\*Address all correspondence to: Pubu Ciren, E-mail: [pbtsering@gmail.com](mailto:pbtsering@gmail.com)

overexposure of PM<sub>10</sub>, crucial information for developing environmental quality standards and analyzing environmental benefits and risks.

Estimating PM concentration from satellite observations has been a hot topic in recent years, owing to the advantage of satellite observations in terms of their large spatial coverage and reasonable temporal resolution. Many empirical models and semiempirical observation-based models were developed to estimate ground PM concentration. Empirical models were based on statistical regressions between aerosol optical depth (AOD) and *in situ* PM measurements, such as the simple linear regression models,<sup>4,5</sup> and multiple linear regression models taking into account the impacts of boundary, temperature,<sup>6</sup> relative humidity (RH), and aerosol vertical distribution.<sup>7,8</sup> Semiempirical observation-based models considered the effects of aerosol characteristics, such as hygroscopic growth, particle mass extinction efficiency, and size distribution.<sup>9,10</sup>

As for the human health impact assessment, many previous studies have been carried out and shown that the level of PM<sub>10</sub> is associated with the rate of death from cardiovascular and respiratory illnesses.<sup>11,12</sup> Gauderman et al.<sup>13</sup> proposed a cross-sectional and cohort study method, which was a new approach for studying the exposure–response relationship between air pollution and illnesses. Over China, Aunan and Pan<sup>14</sup> calculated the concentration response coefficients for diseases caused by air pollution by meta-analysis, and An et al.<sup>15</sup> assessed the human exposure to PM<sub>10</sub> in China based on ground observation data.

However, some shortfalls still exist in those traditional approaches to assess the human health impact caused by air pollution. One of those is that the method suggested in these previous studies typically relied upon air pollution data from ground-based observations, which tend to be clustered in areas of poor air quality and high population. Using the ground-based observations alone is likely to be inadequate to represent the spatial variability of air pollution concentration, which may lead to overestimation of the impact of air pollution on human health. Some research<sup>16,17</sup> calculated PM<sub>10</sub> concentration by spatial interpolation of ground-based observation; however, due to the poor representative and irregular distribution of those ground-based stations, these methods are constrained by physiochemical models and may not generate satisfactory results especially in complex terrain areas.<sup>18</sup> Although it is a good solution to calculate the air pollution concentration using a surface model, most models are only suitable for forecasting short-term diffusion of air pollution in small areas.<sup>19,20</sup> Estimating the air pollution concentration over a long-term series in a large area like China with a surface model is a rather difficult task.

To this end, an approach by using moderate resolution imaging spectroradiometer (MODIS) Aerosol Product from 2010 to 2014 to estimate PM<sub>10</sub> concentration is proposed. First of all, compared with the inversion from instantaneous observations with a short time series, the method proposed in this paper could improve the correlation between surface PM<sub>10</sub> concentration and satellite-derived AOD, and avoid inconsistent results caused by instantaneous atmospheric vertical instability and different atmosphere conditions. Second, the impact of PM<sub>10</sub> on human health is also a long-term process except for some extreme circumstances. Hence, reliability is much higher when long time series data are used. Furthermore, PM<sub>10</sub> derived from satellite observations provides a better spatial coverage. It monitors not only the regions around the ground observation stations, but also the areas that are usually lacking observations. Finally, by obtaining the spatial distribution of the population in China, population density is also taken into consideration when assessing the impact of PM<sub>10</sub> on human health through a population-weighted PM<sub>10</sub> exposure model.

The study in this paper consists of three parts. First of all, the impact of aerosol scalar heights and RH on the correlation between MODIS-retrieved AOD and ground PM<sub>10</sub> concentration was analyzed to derive an empirical model to estimate ground PM<sub>10</sub> concentration from satellite-derived AOD. Second, the annual average impact of PM<sub>10</sub> on human health over China from 2010 to 2014 was assessed by using a dose response model, and the spatial distribution of PM<sub>10</sub> exposure risks in China was obtained by analyzing both the distribution of PM<sub>10</sub> concentration and the population. Finally, the validation of satellite-derived PM<sub>10</sub> was analyzed, the advantages of using long-term satellite observations data were discussed, and different evaluation methods were compared.

## 2 Data and Methods

### 2.1 Study Area

China is located in the east of Asia and the west of the Pacific; its climate is significantly affected by both continent and ocean. As a result of its complex terrain, both temperature and precipitation exhibit a complex spatial pattern. Similarly, land-use type in China has a large variability. For instance, sandy deserts and Gobi are mainly located in northwestern China, arable land is the dominant land type in the eastern plain, grassland scatters over the northern part of Inner Mongolia, and forest land is mainly in the northeastern and southwestern China. In addition, the economic development in China is also regionally imbalanced. Eastern areas are more economically developed than western China. Consequently, population density is higher in Yangtze River Delta, Pearl River Delta, and the Bohai Rim Economic Circle, and lower in western China.

With the rapid economic development, air pollution has become one of the top environmental concerns in China.<sup>21</sup> The growing demand for energy and the increasing number of motor vehicles and fast industrialization have led to a serious deterioration in air quality and consequent serious negative effects on human health and ecosystems. In some parts of China, due to the overlaying of different kinds of pollutants, air pollution is more serious over cities and industrial zones. Environmental protection in China is facing huge challenges and becoming more urgent.

### 2.2 Data Collection and Processing

In this research, NASA MODIS C5.1 daily Aerosol Level-2 Product MOD04, over the time period from 2010 to 2014, was used to estimate PM<sub>10</sub> concentration. The data are produced at a spatial resolution of  $10 \times 10 \text{ km}^2$ .<sup>22</sup> We first extracted the valid AOD [aerosol optical thickness at 0.55 micron for both ocean (best) and land (corrected) with best quality data (quality flag = 3)] from MOD 04 daily Aerosol Product; the valid range of this data is from  $-0.05$  to  $5.0$ . The AOD was derived from the Dark Target algorithm.<sup>23</sup> Due to the limitation of the Dark Target algorithm,<sup>24</sup> some data over bright areas and cloudy areas were missing. To deal with this problem, we calculated the missing AOD by integral averaging the value of the day before and the day after. Then we obtained the monthly average AOD and annual average AOD based on the daily Aerosol Product.

After that, we collected PM<sub>10</sub> annual average concentration measured over 228 Chinese cities from 2010 to 2014. The annual average PM<sub>10</sub> concentration in each city is the mean value of all the monitoring stations in both urban and suburban areas in this city. The average PM<sub>10</sub> concentration measured in these 228 Chinese cities can be classified into two groups, one group was used for establishing the exponential model, and the other group was used for estimating validations of satellite-derived PM<sub>10</sub> concentration. In this paper, 176 were used to establish the empirical model, and the others were used to evaluate the validation of the model. Monthly average temperature and actual vapor pressure data from 2010 to 2014 were acquired from 194 international exchange meteorological stations in China. And monthly average aerosol scale height was obtained from 98 solar radiation observation stations in China over the time period from 2010 to 2014.

### 2.3 Methodology

#### 2.3.1 Relationship between aerosol optical depth and ground PM<sub>10</sub> mass concentration

##### *Estimating ground aerosol mass concentrations from aerosol optical depth.*

Since the ground PM<sub>10</sub> concentration is defined as the surface concentration of the particles, while the AOD retrieved from satellite observations corresponds to total column concentration of particles under ambient RH, the direct correlation between satellite-based AOD and the ground concentration of PM<sub>10</sub> is relatively low and is influenced by humidity. Due to the hygroscopic growth of aerosols, to accurately estimate the ground PM<sub>10</sub> concentration from satellite-retrieved AOD, RH has to be taken into account. According to the empirical relationship

derived by White and Roberts<sup>25</sup> and Li et al.,<sup>7</sup> the aerosol extinction coefficient ( $\beta_0$ ) is defined as follows:

$$\beta_0 = \rho \times f(\text{RH}) = \rho \times \frac{1}{1 - \text{RH}}, \quad (1)$$

where  $\beta_0$  is the aerosol extinction coefficient,  $\rho$  is the mass concentration and RH is the relative humidity.

In addition, the aerosol extinction coefficient is also a function of height. The variation of the aerosol extinction coefficient ( $\beta_z$ ) with the height can be described as an exponential function:<sup>10</sup>

$$\beta_z = \beta_0 \times e^{-\frac{z}{\text{ASH}}}, \quad (2)$$

where ASH is the aerosol scaling height and  $z$  is the height.

Since the AOD is an integral of the aerosol extinction coefficient in the total column,

$$\text{AOD} = \int_0^{\infty} \beta_z dz = \int_0^{\infty} \beta_0 \times e^{-\frac{z}{\text{ASH}}} dz = \text{ASH} \times \beta_0. \quad (3)$$

Therefore, the ground aerosol mass concentration (AMC) can finally be written as

$$\text{AMC} = \frac{\beta_0}{f(\text{RH})} = \frac{\text{AOD}}{\text{ASH}} \times (1 - \text{RH}). \quad (4)$$

The spatial distribution of the monthly mean ASH was obtained from 98 solar radiation observation stations in China over the time period from 2010 to 2014 by using Kriging interpolation. RH was calculated with the modified Magnus equation.<sup>26</sup>

$$\text{RH} = \frac{e_a}{e_0(T)} \times 100, \quad (5)$$

$$e_0(T) = 610.78 \times e^{\frac{17.269(T-273.16)}{T-35.86}}, \quad (6)$$

where  $e_a$  is the actual vapor pressure and  $e_0(T)$  is the saturation vapor pressure at air temperature  $T$ . It is obvious that knowledge of the spatial distribution of both  $T$  and  $e_a$  are required to generate the RH spatial distribution over China. To this end,  $e_a$  was obtained through interpolation of the monthly mean vapor pressure data in China by using Kriging interpolation. From Eq. (6), it is seen that to obtain the spatial distribution of the saturated vapor pressure, air temperature has to be known. First of all, monthly mean air temperature data from 183 meteorological stations in China are converted to air temperature at sea level according to the following definition:

$$T_2 = T_1 + \frac{0.65h}{100}, \quad (7)$$

where  $T_1$  is the measured air temperature at meteorological stations,  $T_2$  is the temperature at virtual sea level, and  $h$  is the altitude, which is calculated with a digital elevations model. Since the variation of air temperature at the same level is considered as continuous, the air temperature at sea level was calculated through Kriging interpolation. Second, the actual air temperatures were obtained by converting the interpolated air temperature at virtual sea level back to actual elevation with Eq. (7). Finally, by combining Eqs. (4), (5), and (6), the monthly mean surface aerosol mass concentration was estimated.

**Relationship between ground PM<sub>10</sub> concentration and ground AMC.** PM<sub>10</sub> is microscopic solid or liquid matter suspended in the Earth's atmosphere, with an aerodynamic diameter <10  $\mu\text{m}$ . AMC includes aerosols with various sizes, while PM<sub>10</sub> accounts for only the

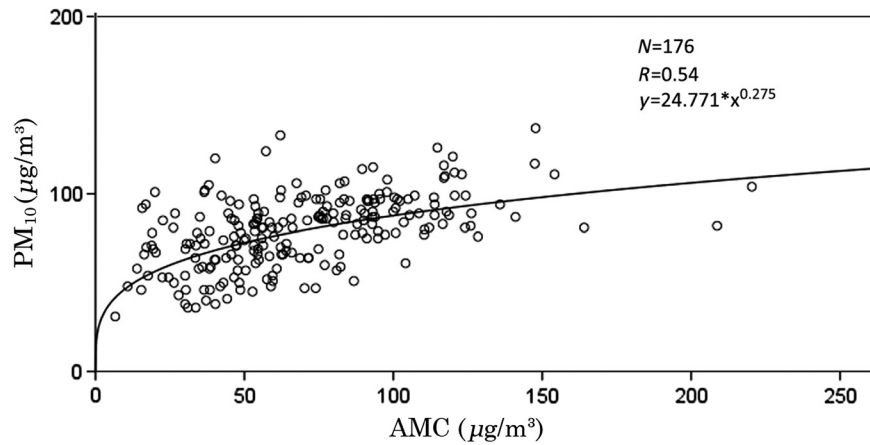


**Fig. 1** The relationship between aerosol mass concentration and ground PM<sub>10</sub> mass concentration.

aerosols with sizes  $<10 \mu\text{m}$ . To obtain the PM<sub>10</sub> concentration from AMC, we first selected the PM<sub>10</sub> annual average concentration observed over 176 Chinese cities from 2010 to 2014. Note that the PM<sub>10</sub> annual concentration for each city is the mean value of all the monitoring stations in both urban and suburban areas. Then we compared the annual average AMC with the annual average surface monitors located in the grid of the remote sensing data and analyzed the regression relation between them. It is found that there is an exponential relationship between annual average ground AMC from 2010 to 2014 and corresponding ground PM<sub>10</sub> mass concentration over these cities. The derived relationship is given and shown in Fig. 1.

### 2.3.2 Distribution of population in China

Statistical population data from a 10-year population census in China are usually given for each administrative district, that is to say, the data are usually at the county level. In addition, the process of urbanization in China has made the population more mobile. Therefore, the spatial and temporal resolution of the statistical population data is too low to be suitable for the purpose of our study. To tackle this problem, a spatial distribution model of the population was adopted to obtain a grid map of spatial distribution of the population over China.

Based on the assumption that a strong correlation exists between the total population and land-use type, a raster population model<sup>27</sup> was adopted and given as

$$\text{POP}_{i,j} = P_{i,r} \times \frac{V_{j,r}}{\sum_{j=1}^k V_{j,r}} + P_{i,u} \times \frac{V_{j,u}}{\sum_{j=1}^k V_{j,u}}, \quad (8)$$

where  $\text{POP}_{i,j}$  is the total population of  $j$ 'th pixel in the  $i$ 'th administrative district,  $P_{i,r}$  is the total rural population in this area,  $P_{i,u}$  is the urban population in this area,  $k$  is the total number of pixels in this area, and  $V_{j,u}$  is the coefficient of the urban population, which is calculated by a distance attenuation exponential model based on the scale of the urban city.  $V_{j,r}$  is the coefficient of the rural population in this area, which is calculated with a weighted linear model. In this model, the indicators are selected according to the relationship between population in various types of agricultural land, and the weighting coefficients are determined by the correlation between land use and population.

### 2.3.3 Population-weighted exposure model

PM<sub>10</sub> human health risks assessment is a process that quantitatively describes the impact of PM<sub>10</sub> exposure on human health. The concentration of PM<sub>10</sub> alone is not able to fully describe the human exposure level since PM<sub>10</sub> concentration and spatial distribution of human population are often inconsistent. The spatial variability of both human population and PM<sub>10</sub> concentration

should be taken into account when assessing health risks. Therefore, a population-weighted exposure model<sup>15,28</sup> was adopted to quantify the PM<sub>10</sub> exposure level.

$$P_{\text{wel}} = \frac{\sum (P_i \times C_i)}{\sum P_i}, \quad (9)$$

where  $i$  is the number of the grid,  $P_i$  is the total population in  $i$ 'th grid, and  $C_i$  is the PM<sub>10</sub> concentration in the  $i$ 'th grid. The model is affected by both population density and PM<sub>10</sub> concentration in the grid.

### 2.3.4 PM<sub>10</sub> human health risks and losses assessment

Human health risks and losses caused by PM<sub>10</sub> exposure are evaluated quantitatively by using the dose-response model. The studies by WHO showed that the relative risk (RR) of the health endpoints has a logarithmic relationship with PM<sub>10</sub> concentration,<sup>29</sup> which is defined as

$$\text{RR} = \frac{e^{\alpha+\beta C}}{e^{\alpha+\beta C_0}} = e^{\beta \cdot (C-C_0)}. \quad (10)$$

and the human health effect of the air pollution model is defined as

$$E = E_0 \times \text{RR} = E_0 \times e^{\beta(C-C_0)}, \quad (11)$$

where  $E$  is the incidence of health endpoints at an actual concentration of PM<sub>10</sub>,  $C_0$  is the reference concentration of PM<sub>10</sub>, which means the highest concentration that is harmless to human health,  $E_0$  is the incidence of health endpoints at a reference concentration of PM<sub>10</sub>,  $\beta$  is the exposure-response relationship coefficient, and  $C$  is the actual concentration of PM<sub>10</sub>. According to WHO standards,<sup>26</sup> the annual average reference concentration of PM<sub>10</sub> is 20  $\mu\text{g}/\text{m}^3$ . Health losses caused by PM<sub>10</sub> exposure are then calculated as

$$\Delta E = E - E_0. \quad (12)$$

The total health losses model for all health endpoints is given as

$$E_{\text{SUM}} = \sum_{i=1}^n (E - E_0) \cdot P_e, \quad (13)$$

where  $E_{\text{SUM}}$  is the total health losses,  $n$  is the number of health endpoints, and  $P_e$  is the total number of the population that is exposed to PM<sub>10</sub> pollution. Overexposure of PM<sub>10</sub> leads to an increased rate of premature death, cardiopulmonary, and cardiovascular diseases. Therefore, in this study, total mortality, respiratory diseases, and cardiovascular diseases are treated as health endpoints. The health effects to PM<sub>10</sub> concentration is related to health endpoints through the exposure-response relationship as shown in Eqs. (10) and (11).

Exposure-response coefficient ( $\beta$ ) is defined as the increase of rate of a health endpoint for a 10  $\mu\text{g}/\text{m}^3$  increase in PM<sub>10</sub> concentration. It is clear that determination of the exposure-response coefficient is a crucial step to accurately evaluate the human health risks and losses caused by the exposure to PM<sub>10</sub>. In this study, the exposure-response coefficients ( $\beta$ ) from previous studies<sup>30-36</sup> were used, and are shown in Table 1.

Baseline health statistical data show the mortality or morbidity of each health endpoint; they are obtained through sample surveys. In this study, the annual average mortality or morbidity statistical data are from *China Health Statistics Yearbook*.<sup>37-40</sup> Mortality in urban and rural areas, and morbidities of respiratory and cardiovascular diseases in the total population are shown in Table 2.

**Table 1** Exposure response coefficient.

Health endpoints	Demographic	Exposure-response coefficient
Mortality	Adults ( $\geq 30$ years old)	0.0043
Respiratory diseases	Whole population	0.0013
Cardiovascular diseases	Whole population	0.0013

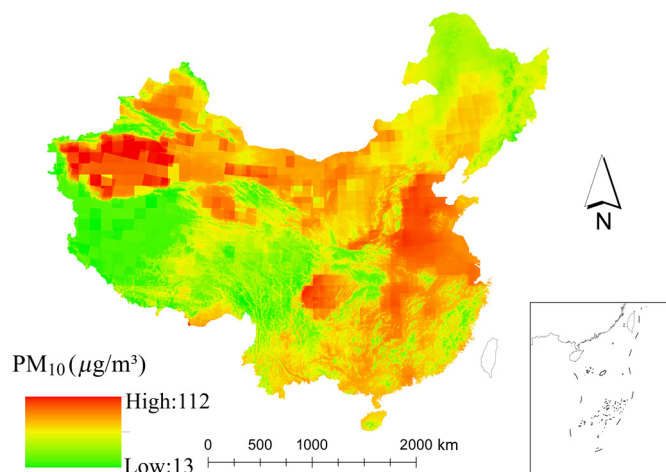
**Table 2** Baseline health statistical data (‰).

Health endpoints	Details	Baseline health statistical data (‰)
Mortality	Urban areas	3.37
	Rural areas	3.57
	<b>Mean</b>	<b>3.52</b>
Respiratory diseases	Acute upper respiratory infections	38.02
	Pneumonia	1.06
	Bronchopneumonia	4.10
	<b>Total</b>	<b>43.18</b>
Cardiovascular diseases	Heart disease	10.68
	Hypertension	31.36
	Cerebrovascular disease	5.85
	<b>Total</b>	<b>47.89</b>

### 3 Results

#### 3.1 Spatial Distribution of PM<sub>10</sub> in China

The annual average PM<sub>10</sub> spatial distribution from 2010 to 2014 derived from the relationship between ground PM<sub>10</sub> concentration and satellite-derived AOD is shown in Fig. 2. The spatial resolution of the map is  $10 \times 10$  km<sup>2</sup>. It is seen that the highest annual average PM<sub>10</sub>

**Fig. 2** Annual average PM<sub>10</sub> in China from 2010 to 2014.

concentration is mainly concentrated in Northern China, the Sichuan Basin, and Taklimakan Desert regions, where annual average PM<sub>10</sub> concentration is  $>100 \mu\text{g}/\text{m}^3$ . The northwestern, the middle and lower reaches of the Yangtze River, and Inner Mongolia, Shaanxi, Shanxi, and some other provinces in northern China are as high as  $80 \mu\text{g}/\text{m}^3$ . In the northeastern area, Liaoning and Jilin, the annual average PM<sub>10</sub> concentration is  $\sim 70 \mu\text{g}/\text{m}^3$ . In southwestern and southern China, PM<sub>10</sub> concentration is  $\sim 60 \mu\text{g}/\text{m}^3$ . Over the Tibetan Plateau, Fujian and Heilongjiang province, PM<sub>10</sub> concentration has the lowest value. In general, concentration is the highest in the northern zone, followed by the central region, and the concentration is lowest in southern China and the Tibetan Plateau.

### 3.2 Spatial Distribution of Population in China

Figure 3 shows the annual average population density over China from 2010 to 2014 in a resolution of 10 km. In general, the permanent population of China is mainly concentrated in the eastern coastal area. Population density in northern China, southern China, and the middle and lower reaches of Yangtze River is much larger than that in western China. Population density in the plain and basin areas is overall higher, while it is much lower in mountainous and plateau regions. Areas along rivers and the coast are more densely populated.

### 3.3 Population-Weighted PM<sub>10</sub> Exposure Level

To accurately assess the impact of PM<sub>10</sub> exposure on human health, the distribution of PM<sub>10</sub> has to be combined with the distribution of the population. Therefore, according to the population-weighted PM<sub>10</sub> exposure model, given in Eq. (9), population-weighted PM<sub>10</sub> exposure levels are calculated and are shown in Fig. 4. It is clearly seen that, in both northern China and the Sichuan Basin regions, which are highly populated and industrialized and have a higher annual average PM<sub>10</sub> concentration from 2010 to 2014, the population-weighted PM<sub>10</sub> exposure level is even higher; it can reach up to  $100 \mu\text{g}/\text{m}^3$ . In the middle and lower reaches of the Yangtze River, from Wuhan to Nanjing, the population-weighted PM<sub>10</sub> exposure level is as high as  $\sim 85 \mu\text{g}/\text{m}^3$ . In northeastern, southern, and southwestern China, population-weighted PM<sub>10</sub> exposure level is  $\sim 65 \mu\text{g}/\text{m}^3$ , much lower than that in the northern China and the Yangtze River region. However, most western and northwestern regions have a very low population-weighted exposure level as a result of both less population and underdeveloped industry.

### 3.4 PM<sub>10</sub> Human Health Losses in China

Finally, according to human health effects of the PM<sub>10</sub> model, as shown in Eqs. (12) and (13), the human health losses of each health endpoint resulting from PM<sub>10</sub> exposure are evaluated.

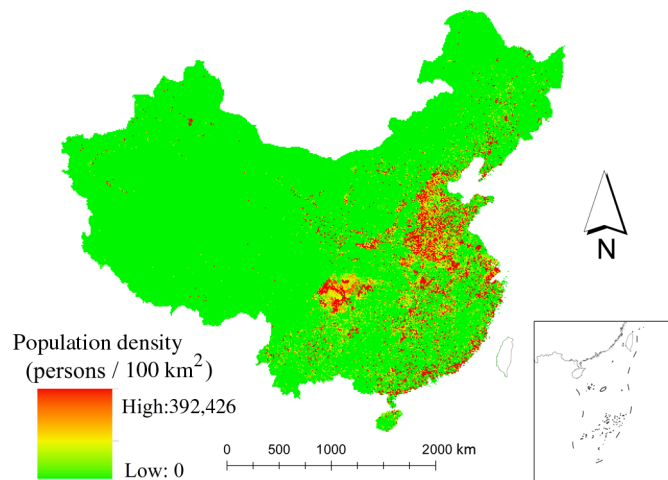


**Fig. 3** Annual average population density in China from 2010 to 2014.

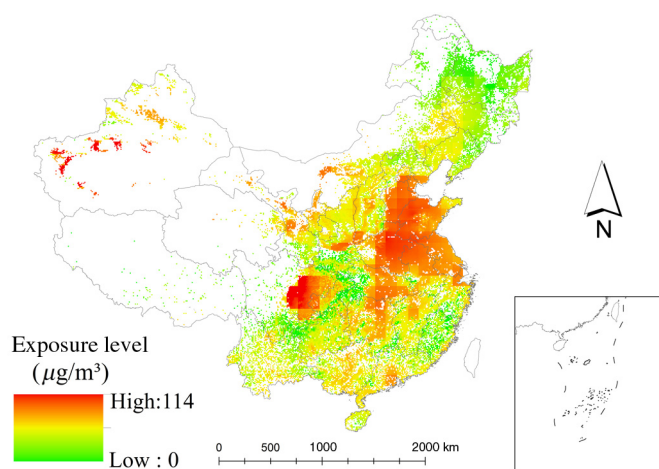


**Fig. 4** Annual average population-weighted PM<sub>10</sub> exposure level from 2010 to 2014.

It is found that, from 2010 to 2014, exposure to PM<sub>10</sub> air pollution has caused a negative effect on health for ~6.9 million people in China every year. Among them, there are 0.9 million cases of death and 6.0 million cases of acute health diseases. More specifically, ~3.5 million people suffer from acute respiratory illness, and 2.5 million people suffer from acute cardiovascular diseases due to the exposure to PM<sub>10</sub>.

## 4 Discussion

### 4.1 Validation of Satellite-Derived PM<sub>10</sub>

The uncertainties of the satellite-derived PM<sub>10</sub> lead to the uncertainties of the human health impact resulting from PM<sub>10</sub> exposure. To estimate the validation of the satellite-derived PM<sub>10</sub> concentration, the annual average PM<sub>10</sub> concentration measured in 228 Chinese cities was first analyzed using cluster analysis. Then these ground measured data were divided into four categories. They represent four PM<sub>10</sub> pollution levels, and the PM<sub>10</sub> concentration is significantly different in each category. To estimate the overall validation of the satellite-derived PM<sub>10</sub>, we first selected 52 of them as the samples according to the method of stratified sampling.<sup>41</sup> Note that 52 is the minimum number of samples when these cities were divided into four categories. Then we compared the annual average of ground-based PM<sub>10</sub> concentration with the annual average of satellite-derived PM<sub>10</sub> concentration of these 52 samples from 2010 to 2014, as shown in Fig. 5. A linear relationship exists between the satellite-derived PM<sub>10</sub> and ground-based PM<sub>10</sub>; the correlation coefficient is as high as 0.83, root mean square error is 19.27, relative standard deviation is 12.66%, and mean absolute percentage error (MAPE) is only 7.70%. High correlation and low MAPE indicates the applicability and reliability of PM<sub>10</sub> concentration derived from MODIS data. The mean bias of the concentration of PM<sub>10</sub> is <10 µg/m<sup>3</sup> based on the accuracy of MODIS AOD retrievals over land. The corresponding transferred bias for the relative risks from exposure to PM<sub>10</sub> is <0.01 according to the PM<sub>10</sub> human health impact model and the bias of negative cases from PM<sub>10</sub> exposure is <0.2 million.

### 4.2 Advantages of Satellite-Derived PM<sub>10</sub> in Estimating Human Health Impact

The correlation between short-term satellite data and ground PM is relatively low in some meteorological conditions, especially when troposphere air changes. Tian and Chen<sup>42</sup> found that the instantaneous satellite data were poorly related to the ground-based PM<sub>2.5</sub> concentration due to changes in meteorological conditions. Hutchison<sup>43</sup> indicated that a stronger correlation can be obtained by averaging longer timescales' satellite observation data and ground-based PM<sub>2.5</sub> data. In this study, we obtained annual average AOD from MODIS Aerosol Product data for the years from 2010 to 2014 and annual average ground PM<sub>10</sub> observations to avoid the problem of low correlation

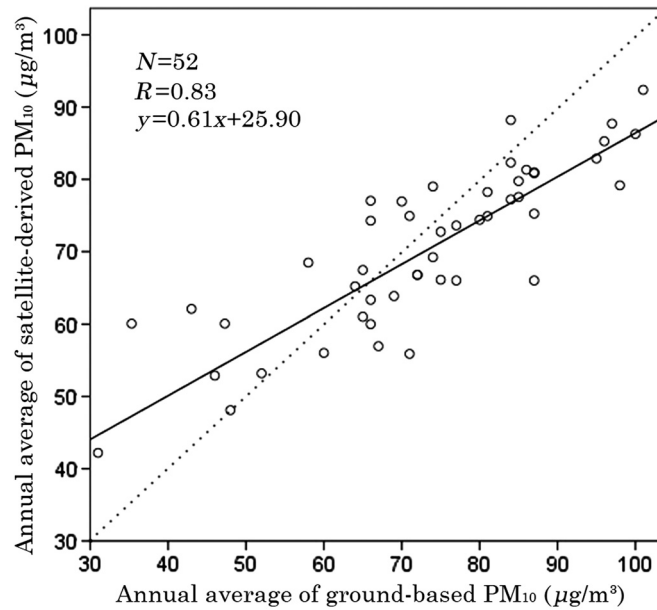


**Fig. 5** Comparison of annual average of ground-based PM<sub>10</sub> concentration and satellite-derived PM<sub>10</sub> concentration.

between AOD and ground PM<sub>10</sub> concentration caused by instantaneous atmospheric vertical instability and different atmosphere conditions. Furthermore, the impact of PM<sub>10</sub> exposure on human health is a long-term process, and research on human health impact based on long-term satellite-derived PM<sub>10</sub> data can improve the accuracy of the results.

Correlating the human health impact with long-term PM<sub>10</sub> concentration derived from satellite observations has many advantages. Currently, most works on the assessment of air pollution to human health in a certain region are usually based on the average ground-based observations data.<sup>44,45</sup> It is known that the air quality monitoring stations are mainly located in the areas where PM<sub>10</sub> concentration is higher, such as urban areas. Consequently, PM<sub>10</sub> concentration and subsequent human health risks and losses are overestimated. Although some studies<sup>46,47</sup> used the interpolated PM<sub>10</sub> concentration from ground-based observations to access the human health risks and losses, these methods are constrained by physiochemical models and may not generate accurate results in complex terrain areas.<sup>18</sup> Surface models<sup>20</sup> based on GIS and ground-based observations could provide more accurate results of PM<sub>10</sub> concentration; however, they are usually not suitable for calculating long-term diffusion of air pollution in large areas. In our study, PM<sub>10</sub> concentration derived from satellite observations can be considered more realistic than the above methods, since no direct interpolation on PM<sub>10</sub> concentration is involved.

The distribution of population is another factor that has to be taken into account to accurately assess the impact of air pollution on human health. However, the statistical population data from census are given for each administrative district and do not provide sufficient spatial resolution<sup>24</sup> for the purpose of this study. To this end, based on the correlation between the total population and land-use type, we generated a population distribution map with a resolution of 10 km. Such a distribution map demonstrates the spatial variations of population over China. In addition, unlike traditional human health assessment methods, which overlay the *in situ* PM<sub>10</sub> concentrations data over statistical population data given by the administrative district, we obtained the spatial distribution of human health risks in China by analyzing the spatial distribution of both PM<sub>10</sub> concentration and population. To show the advantages of the approach used in our study, we calculated the human health risks and losses based on both the satellite observations data and ground-based observations data. Comparison of the results of the two approaches is given in Figs. 6 and 7.

It is shown in Fig. 6 that relative risks based on satellite observations are generally lower than that based on ground-based observations in most provinces, except for Shanghai, which includes more highly populated areas, and Hainan, Guangdong, Guangxi, which are located in the

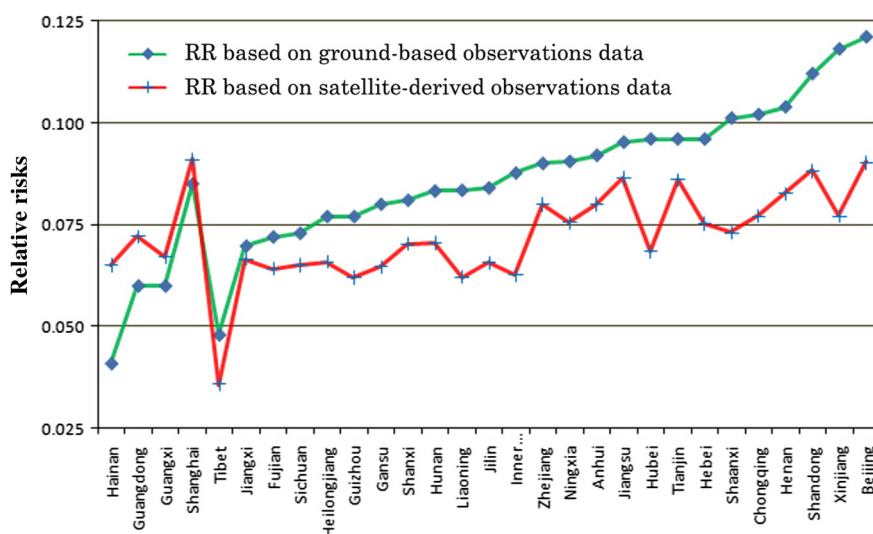


**Fig. 6** Comparison of relative risk based on ground-based observations data with relative risk based on satellite observations data at a provincial scale.

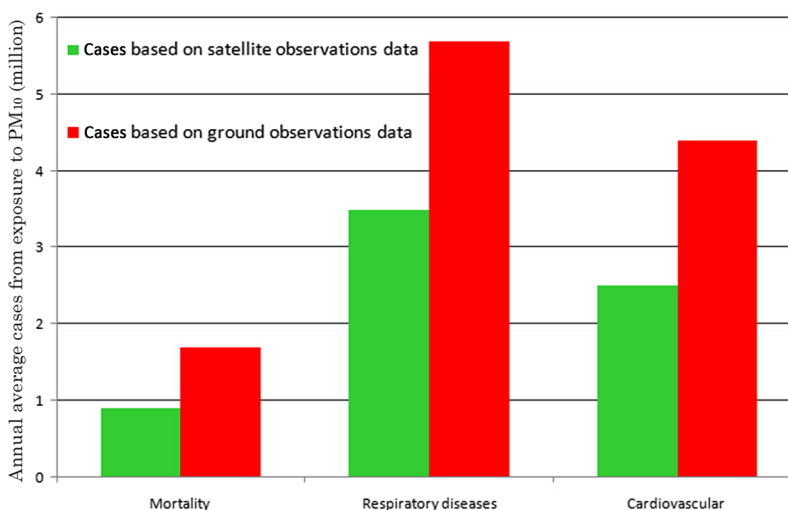


**Fig. 7** Comparison of human health losses based on ground-based observations data with losses based on satellite observations data.

subtropical monsoon climate zone. Humid weather and complex atmosphere conditions lead to a lower accuracy in estimating PM<sub>10</sub> concentration in these regions. For all other provinces, relative risk by PM<sub>10</sub> exposure based on satellite observations is lower than that based on ground observations data. As for the annual average human health losses caused by PM<sub>10</sub> exposure from 2010 to 2014, as shown in Fig. 7, the total number of cases of detrimental health impact from PM<sub>10</sub> pollution estimated with ground-based PM<sub>10</sub> observations is 10.21 million, which is much larger than the estimation with the method proposed in our study.

## 5 Conclusions

In this study, an empirical model to estimate ground PM<sub>10</sub> mass concentration from AOD was first investigated, and the effect of PM<sub>10</sub> exposure on human health in China was then assessed with the dose-response model. Compared with other existing studies, our study has improvements in three aspects. First of all, long-term remote sensing data were used instead of ground-based observations to estimate the spatial distribution of PM<sub>10</sub> concentration in order to avoid

the problem of low correlation between AOD and ground PM<sub>10</sub> concentration, which is caused by instantaneous atmospheric vertical instability and different atmosphere conditions. Second, a map of spatial distribution of the population was generated by using the relationship between population and land-use type to avoid the problems associated with the statistics population data from census, such as low spatial and temporal resolution, since the statistics population data are usually at the administrative county level and its update cycle is long, ~10 years. Finally, taking into account the spatial distribution of both PM<sub>10</sub> concentration and population to assess the human health impact by PM<sub>10</sub> exposure gave more accurate results for areas where a high PM<sub>10</sub> concentration is associated with a low population. A comparison between the satellite-derived PM<sub>10</sub> and ground-based PM<sub>10</sub> indicated the validation of the method proposed in this research, and a comparison between the methods based on ground-based observations data and satellite observations data indicated that using long-term satellite observations has great potential and advantages in human health impact assessment.

In a variety of atmospheric particulate pollution, PM<sub>2.5</sub> poses the greatest risks to human health and shows stronger epidemiological links with human health. However, due to lack of PM<sub>2.5</sub> monitoring data, since PM<sub>2.5</sub> concentration was not included in the air quality standard in China until February 2012, only PM<sub>10</sub> is chosen as the main pollutant when assessing the risks of PM to human health in this paper. In future studies, we will take PM<sub>2.5</sub>, ozone, nitrogen oxides, sulfides, and some other air pollutants into consideration. The impact of air pollution on human health is a long-term integrated process; how to integrate the various components of air pollution on human health and determine the relationship between the different components will be another challenge.

## Acknowledgments

This study was supported by Major Program of National Social Science Foundation of China (11&ZD157). Thanks for the reviewers' suggestions.

## References

1. World Health Organization, *The World Health Report 2002: Reducing the Risks, Promoting Healthy Life*, World Health Organization, Geneva (2002).
2. A. J. Cohen et al., "The global burden of disease due to outdoor air pollution," *J. Toxicol. Environ. Health A* **68**(13–14), 1301–1307 (2005).
3. Q. Zhang and R. Crooks, *Toward an Environmentally Sustainable Future: Country Environmental Analysis of the Peoples Republic of China*, Asian Development Bank, Manila (2013).
4. D. A. Chu et al., "Global monitoring of air pollution over land from the Earth Observing System-Terra moderate resolution imaging spectroradiometer (MODIS)," *J. Geophys. Res.* **108**(D21), 1261–1270 (2003).
5. J. Wang and S. A. Christopher, "Intercomparison between satellite-derived aerosol optical thickness and PM<sub>2.5</sub> mass: implications for air quality studies," *Geophys. Res. Lett.* **30**(21), 2095 (2003).
6. P. Gupta and S. A. Christopher, "Particulate matter air quality assessment using integrated surface, satellite, and meteorological products: multiple regression approach," *J. Geophys. Res.* **114**(D14), 233–245 (2009).
7. C. Li et al., "Application of MODIS satellite products to the air pollution research in Beijing," *Sci. China D Earth Sci.* **48**(Suppl. 2), 209–219 (2005).
8. X. Liu et al., "Influences of relative humidity and particle chemical composition on aerosol scattering properties during the 2006 PRD campaign," *Atmos. Environ.* **42**(7), 1525–1536 (2008).
9. E. Emili et al., "PM<sub>10</sub> remote sensing from geostationary SEVIRI and polar-orbiting MODIS sensors over the complex terrain of the European Alpine region," *Remote Sens. Environ.* **114**(11), 2485–2499 (2010).
10. C. Lin et al., "Using satellite remote sensing data to estimate the high-resolution distribution of ground-level PM<sub>2.5</sub>," *Remote Sens. Environ.* **156**, 117–128 (2015).

11. J. M. Samet et al., "Fine particulate air pollution and mortality in 20 US cities, 1987-1994," *N. Engl. J. Med.* **343**(24), 1742–1749 (2000).
12. L. Ma et al., "Effects of airborne particulate matter on respiratory morbidity in asthmatic children," *J. Epidemiol.* **18**(3), 97–110 (2008).
13. W. J. Gauderman et al., "Association between air pollution and lung function growth in southern California children: results from a second cohort," *Am. J. Respir. Crit. Care Med.* **166**(1), 76–84 (2002).
14. K. Aunan and X. C. Pan, "Exposure-response functions for health effects of ambient air pollution applicable for China—a meta-analysis," *Sci. Total Environ.* **329**(1), 3–16 (2004).
15. X. An et al., "Assessment of human exposure level to PM<sub>10</sub> in China," *Atmos. Environ.* **70**, 376–386 (2013).
16. D. E. Abbey et al., "Long-term inhalable particles and other air pollutants related to mortality in nonsmokers," *Am. J. Respir. Crit. Care Med.* **159**(2), 373–382 (1999).
17. M. Jerrett et al., "Spatial analysis of air pollution and mortality in Los Angeles," *Epidemiology* **16**(6), 727–736 (2005).
18. O. Hertel et al., "Human exposure to outdoor air pollution (IUPAC technical report)," *Pure Appl. Chem.* **73**(6), 933–958 (2001).
19. D. T. Shindell et al., "A multi-model assessment of pollution transport to the Arctic," *Atmos. Chem. Phys.* **8**(17), 5353–5372 (2008).
20. J. H. Seinfeld and S. N. Pandis, *Atmospheric Chemistry and Physics: From Air Pollution to Climate Change*, John Wiley & Sons, Hoboken (2012).
21. C. K. Chan and X. Yao, "Air pollution in mega cities in China," *Atmos. Environ.* **42**(1), 1–42 (2008).
22. NASA, "MODIS Aerosol Product," <http://modis.gsfc.nasa.gov/data/dataproduct/mod04.php> (4 July 2015)
23. L. A. Remer et al., "The MODIS aerosol algorithm, products, and validation," *J. Atmos. Sci.* **62**(4), 947–973 (2005).
24. N. C. Hsu et al. "Aerosol properties over bright-reflecting source regions," *IEEE Trans. Geosci. Remote Sens.* **42**(3), 557–569 (2004).
25. W. H. White and P. T. Roberts, "On the nature and origins of visibility-reducing aerosols in the Los Angeles air basin," *Atmos. Environ. (1967)* **11**(9), 803–812 (1977).
26. O. A. Alduchov and R. E. Eskridge, "Improved Magnus form approximation of saturation vapor pressure," *J. Appl. Meteorol.* **35**(4), 601–609 (1996).
27. Y. Mao, A. Ye, and J. Xu, "Using land use data to estimate the population distribution of China in 2000," *GISci. Remote Sens.* **49**(6), 822–853 (2012).
28. X. An et al., "Assessment of human exposure level to PM<sub>10</sub> in China," *Atmos. Environ.* **70**, 376–386 (2013).
29. World Health Organization, *Air Quality Guidelines: Global Update 2005: Particulate Matter, Ozone, Nitrogen Dioxide, and Sulfur Dioxide*, World Health Organization, Geneva (2006).
30. C. A. Pope, III et al., "Lung cancer, cardiopulmonary mortality, and long-term exposure to fine particulate air pollution," *JAMA* **287**(9), 1132–1141 (2002).
31. C. A. Pope, III, M. Ezzati, and D. W. Dockery, "Fine-particulate air pollution and life expectancy in the United States," *N. Engl. J. Med.* **360**(4), 376–386 (2009).
32. T. W. Wong et al., "Air pollution and hospital admissions for respiratory and cardiovascular diseases in Hong Kong," *Occup. Environ. Med.* **56**(10), 679–683 (1999).
33. T. W. Wong et al., "Associations between daily mortalities from respiratory and cardiovascular diseases and air pollution in Hong Kong, China," *Occup. Environ. Med.* **59**(1), 30–35 (2002).
34. G. D. Thurston et al., "Respiratory hospital admissions and summertime haze air pollution in Toronto, Ontario: consideration of the role of acid aerosols," *Environ. Res.* **65**(2), 271–290 (1994).
35. J. Schwartz, "Air pollution and hospital admissions for the elderly in Detroit, Michigan," *Am. J. Respir. Crit. Care Med.* **150**(3), 648–655 (1994).

36. K. A. Miller et al., "Long-term exposure to air pollution and incidence of cardiovascular events in women," *N. Engl. J. Med.* **356**(5), 447–458 (2007).
37. Ministry of Health of China, *China Health Statistics Yearbook 2011*, Peking Union Medical College Press, Beijing (2011).
38. Ministry of Health of China, *China Health Statistics Yearbook 2012*, Peking Union Medical College Press, Beijing (2012).
39. Ministry of Health of China, *China Health Statistics Yearbook 2013*, Peking Union Medical College Press, Beijing (2013).
40. Ministry of Health of China, *China Health Statistics Yearbook 2014*, Peking Union Medical College Press, Beijing (2014).
41. G. W. Imbens and T. Lancaster, "Efficient estimation and stratified sampling," *J. Econom.* **74**(2), 289–318 (1996).
42. J. Tian and D. Chen, "A semi-empirical model for predicting hourly ground-level fine particulate matter (PM<sub>2.5</sub>) concentration in southern Ontario from satellite remote sensing and ground-based meteorological measurements," *Remote Sens. Environ.* **114**(2), 221–229 (2010).
43. K. D. Hutchison, "Applications of MODIS satellite data and products for monitoring air quality in the state of Texas," *Atmos. Environ.* **37**(17), 2403–2412 (2003).
44. W. E. Wilson and H. H. Suh, "Fine particles and coarse particles: concentration relationships relevant to epidemiologic studies," *J. Air Waste Manage. Assoc.* **47**(12), 1238–1249 (1997).
45. M. Brauer et al., "Estimating long-term average particulate air pollution concentrations: application of traffic indicators and geographic information systems," *Epidemiology* **14**(2), 228–239 (2003).
46. T. Bellander et al., "Using geographic information systems to assess individual historical exposure to air pollution from traffic and house heating in Stockholm," *Environ. Health Perspect.* **109**(6), 633 (2001).
47. D. Liao et al., "Ambient particulate air pollution and ectopy—the environmental epidemiology of arrhythmogenesis in women's health initiative study, 1999-2004," *J. Toxicol. Environ. Health A* **72**(1), 30–38 (2008).

**Wen Wang** is an associate professor at the Center for Spatial Information, School of Environment and Natural Resources, Remin University of China. He obtained his PhD from the Institute of Remote Sensing Applications, Chinese Academy of Sciences in 1997. His research interests include remote sensing applications in air pollution and human health impact.

**Tao Yu** is a postgraduate student at the Center for Spatial Information, School of Environment and Natural Resources, Remin University of China. His current research focuses on the inversion model of particulate matter.

**Pubu Ciren** works at IMSG at NOAA/NESDIS/STAR. He is also a guest researcher at the Center for Spatial Information, School of Environment and Natural Resources, Remin University of China. He has over 20 years of experience in atmospheric remote sensing.

**Peng Jiang** is a postgraduate student at the Center for Spatial Information, School of Environment and Natural Resources, Remin University of China.